



Computational Design of Hand-Held VR Controllers Using Haptic Shape Illusion

Eisuke Fujinawa

The University of Tokyo, Bunkyo-ku,
Tokyo, Japan
nawafuji@cyber.t.u-tokyo.ac.jp

Shigeo Yoshida

The University of Tokyo, Bunkyo-ku,
Tokyo, Japan
shigeodayo@cyber.t.u-tokyo.ac.jp

Yuki Koyama

National Institute of Advanced
Industrial Science and Technology
(AIST), Tsukuba, Ibaraki, Japan
koyama.y@aist.go.jp

Takuji Narumi

The University of Tokyo, Bunkyo-ku,
Tokyo, Japan
narumi@cyber.t.u-tokyo.ac.jp

Tomohiro Tanikawa

The University of Tokyo, Bunkyo-ku,
Tokyo, Japan
tani@cyber.t.u-tokyo.ac.jp

Michitaka Hirose

The University of Tokyo, Bunkyo-ku,
Tokyo, Japan
hirose@cyber.t.u-tokyo.ac.jp

ABSTRACT

Humans are capable of haptically perceiving the shape of an object by simply wielding it, even without seeing it. On the other hand, typical hand-held controllers for virtual reality (VR) applications are pre-designed for general applications, and thus not capable of providing appropriate haptic shape perception when wielding specific virtual objects. Contradiction between haptic and visual shape perception causes a lack of immersion and leads to inappropriate object handling in VR. To solve this problem, we propose a novel method for designing hand-held VR controllers which illusorily represent haptic equivalent of visual shape in VR. In ecological psychology, it has been suggested that the perceived shape can be modeled using the limited mass properties of wielded objects. Based on this suggestion, we built a *shape perception model* using a data-driven approach; we aggregated data of perceived shapes against various hand-held VR controllers with different mass properties, and derived the model using regression techniques. We implemented a design system which enables automatic design of hand-held VR controllers whose actual shapes are smaller than target shapes while maintaining their haptic shape perception. We verified that controllers designed with our system can present aimed shape perception irrespective of their actual shapes.

CCS CONCEPTS

•Human-centered computing →Virtual reality; •Computing methodologies →Perception; Shape modeling;

KEYWORDS

Perception; computational design; data-driven; virtual reality

Permission to make digital or hard copies of all or part of this work for personal or classroom use is granted without fee provided that copies are not made or distributed for profit or commercial advantage and that copies bear this notice and the full citation on the first page. Copyrights for components of this work owned by others than the author(s) must be honored. Abstracting with credit is permitted. To copy otherwise, or republish, to post on servers or to redistribute to lists, requires prior specific permission and/or a fee. Request permissions from permissions@acm.org.

VRST '17, Gothenburg, Sweden

© 2017 Copyright held by the owner/author(s). Publication rights licensed to ACM.
978-1-4503-5548-3/17/11...\$15.00
DOI: 10.1145/3139131.3139160

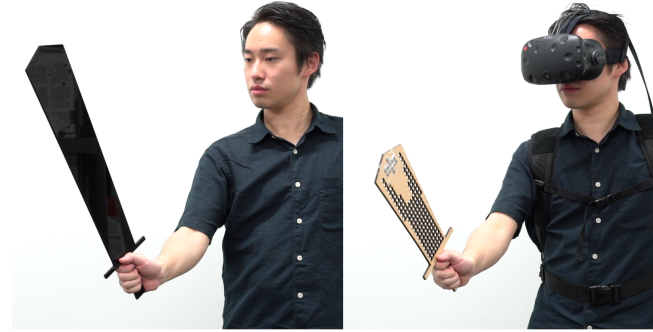


Figure 1: The actual appearance (right) and perceived shape (left) of a hand-held VR controller designed with the proposed system. Though the controller's actual appearance differs from the object's appearance in VR, the user perceives handling the object in VR.

ACM Reference format:

Eisuke Fujinawa, Shigeo Yoshida, Yuki Koyama, Takuji Narumi, Tomohiro Tanikawa, and Michitaka Hirose. 2017. Computational Design of Hand-Held VR Controllers Using Haptic Shape Illusion. In *Proceedings of VRST '17, Gothenburg, Sweden, November 8–10, 2017*, 10 pages.
DOI: 10.1145/3139131.3139160

1 INTRODUCTION

As satisfying virtual reality (VR) hardware has become commercially available, VR has become increasingly popular. VR is expected to be applied to a wide range of fields including medicine, education, advertising, and entertainment. Because the visual quality of VR is now high, developers have shifted their focus to hand-held VR controllers (e.g., Oculus Touch and Playstation Move). Since users handle virtual objects through a hand-held VR controller, the quality of this controller is important for the user.

The appearance of VR controllers is application-dependent, and gives users the impression of controlling different objects. However, humans can estimate the shape of an object with haptic cues, especially when wielding it. Since actual controller shapes are pre-defined, they cannot provide users with appropriate haptic shape

perception specific to wielded objects in VR. Moreover, a contradiction between haptic and visual shape perception can cause a lack of immersion and leads to inappropriate object handling in VR.

One direct approach to reproducing appropriate haptic shape perception is to use an object identical to the virtual object in its shape and the mass properties as a hand-held VR controller. A controller with the identical properties should reasonably lead to the perception that the real and virtual object are the same. However, it is impractical to produce a controller with the same properties as a large virtual object, owing to spatial restrictions due to the limited room space and obstacles (*e.g.*, wall, ceiling, shelf, lamp, etc) in physical environments.

On the other hand, previous studies have investigated a shape illusion in which humans perceive a shape that differs from an object's actual shape [Omosako et al. 2012]. Several studies in ecological psychology have suggested that the main factor in haptic shape perception constitutes the limited mass properties of wielded objects (*e.g.*, the moment of inertia and the static moment [Burton et al. 1990; Kingma et al. 2004; Pagano et al. 1993; Turvey et al. 1998]). This means there is a mapping that relates the specific mass properties to the perceived shape. By taking advantage of this mapping, we can design a hand-held controller with *haptic shape illusion*, with which a user haptically perceives an appropriate shape for an object in VR that is, in reality, smaller and/or lighter.

In this paper, we propose a novel method for designing hand-held VR controllers that appropriately represent visual shape in VR (Figure 1) using a haptic shape illusion. As the first step, we specifically focused on controllers for symmetric planar objects up to 1 m length or width, and implemented a proof-of-concept system in this scope. Our primal target users are VR developers, including indies as well as enterprises. When they demonstrate their content, they can design the dedicated controller which makes their demo or attraction more appealing to the audience. Individual players can also use our system to design an additional dedicated controller for their fun.

Figure 2 shows an overview of our approach. Based on the virtual target shape and physical spatial requirements, a controller design is automatically generated so that its haptic shape perception matches the target shape. To do so, we first build a shape perception model that relates mass properties to haptically perceived shape using a data-driven approach. We aggregate perceived shape data against hand-held VR controllers with different mass properties through perceptual experiments and derive a mapping using regression techniques. Using this mapping, we implement a design system that optimizes the perceived shape of the hand-held controller to be the target shape. The designed model is easily fabricated through a laser cutter or a 3D printer and can be used as a VR controller. We performed a user study using several VR controllers designed by our system to validate that these controllers reproduce the desired shape perception with reduced sizes.

To summarize, our technical contributions include (1) a novel design concept that uses a haptic shape illusion, (2) a data-driven representation of a perceived shape based on the mass properties of a wielded object, and (3) an interactive optimization-guided hand-held VR controller design tool.

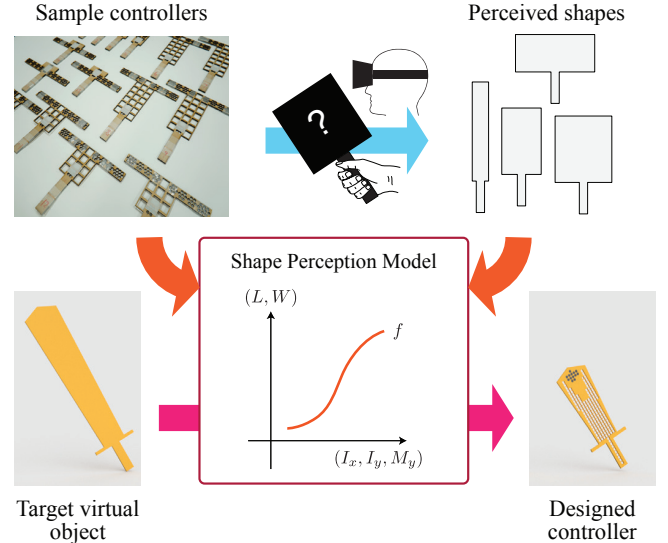


Figure 2: Our framework consists of a precomputation stage and online design sessions. In the precomputation stage, a *shape perception function* that maps mass properties of controllers to their perceived shapes is constructed. This is achieved by utilizing actual data from a perceptual experiment. This function is used in our design system to design a custom hand-held VR controller for a specific target applications.

2 RELATED WORK

Our method is based on established works from various research area, including haptic displays in VR, shape perception in ecological psychology, and computational designs in computer graphics.

2.1 Haptic Displays

Various haptic displays, such as force displays and shape displays, have been developed in order to present rich haptic perceptions to users. Force displays aim to feedback force to the user's hand as it moves using actuators and other mechanisms [Massie and Salisbury 1994; Minamizawa et al. 2007; Nakagawara et al. 2005]. There are varieties in the mechanism sizes that have a trade-off between its structural complexity and the variety of the presented force. Although force displays try to precisely reproduce counter-force, they do not always correspond to the perception of an object's shape as human perception is often nonlinear to stimuli. Some researchers have leveraged this nonlinearity to easily present haptic perception easily [Amemiya et al. 2008; Rekimoto 2013]. However, nonlinear relationships in perception are complicated and unclear. We employ a data-driven approach to model the nonlinear relationship between stimulation and perception.

Instead of rendering force, it is also possible to present local shape outline around a user's hand to present the perception of touching objects. Such haptic displays are called shape displays. For example, Benko et al. [Benko et al. 2016] developed two types of mobile devices to present a local shape to a user's finger, one of which represent the rough shapes by tilting the surface while

the other renders the detailed textures by moving a set of tiny rods. These types of shape displays still have problems with a limited spatial resolution and noticeable latency. While these devices try to present local shape perception when touching a surface, most parts of the mobile controller are not to be touched since users control it with its handle. Therefore, we focused on the overall perception of the whole shape when wielded with its handle while leaving the handle shape alone as it is.

In contrast to the typical haptic displays using dynamic actuators, some methods uses passive haptic properties of a physical object. Azmandian et al. [Azmandian et al. 2016] proposed a method to retargeting passive haptic properties of a single object for handling multiple virtual objects. Their method uses a physical object with identical size with rendered object to present appropriate haptic cue. On the other hand, Zenner et al. [Zenner and Krüger 2017] proposed *Shifty*, a hand-held device that dynamically changes the passive mass properties by shifting weight along with its rendered shape in VR. Their approach can give feeling that the object's length/thickness is changing. However, it does not present appropriate passive properties corresponding to the rendered shape since the mapping from the mass properties to perceived shapes is still unclear. Similar to these approaches, our approach is fully passive; we do not use any actuators to render haptic feedback. Our approach can present various shapes without employing a complicated actuators or mechanisms by switching a controller depending on applications. Although this may sound inconvenient compared to the multi-use controller, preparing the dedicated controllers are very easy since the designed model is easily fabricated through a laser cutter or a 3D printer.

2.2 Haptic Shape Perception

Humans can perceive several spatial and other properties of objects, without seeing them, simply by wielding them. Gibson called this ability as “Dynamic Touch” [Gibson 1966] and many researchers in ecological psychology have worked to clarify its mechanism. Many experiments have been conducted to understand how humans perceive the length of an object. Studies have supported the idea that perceived length and width of the object is mainly related to the moment of inertia (object’s tendency to resist angular acceleration) about the position of the hand [Turvey 1996]. Burton et al. [Burton et al. 1990] suggested that humans can roughly estimate the shape of an object with a handle by blindly wielding it. Pagano et al. [Pagano et al. 1993] showed that the perceived length is in proportion to the maximum principal moment of inertia and is in inverse proportion to the minimum principal moment of inertia. Turvey et al. [Turvey et al. 1998] hypothesized that perceived width is also related to the principal moment of inertia and conducted perceptual experiments using solid rectangular parallelepipeds. Contrary to perceived length, the perceived width was found to be proportional to the minimum principal moment of inertia and is inversely proportional to the maximum principal moment of inertia. Kingma et al. [Kingma et al. 2004] showed that the static moment (equivalent to torque) of the object also contributes to length perception, and that its weight is not related.

Based on these studies, we make the following assumptions about haptic shape perception: (1) the perceived shape of a wielded

object is represented by its length and width and (2) there exists a mapping between the perceived shapes and specific mass properties, *i.e.*, the principal moment of inertia and the static moment about the handle position. Using this mapping, we propose a novel method for designing a VR controller with a desired shape perception. As far as we know, there have been no previous attempt to explicitly utilize this haptic shape perception model for engineering purposes, *i.e.*, to design hand-held VR controllers.

2.3 Computational Design and Data-Driven Methods

Digital fabrication devices such as 3D printers or laser cutters have become widely available, increasing the importance of accessible design tools for functional objects. Recent studies in computer graphics have presented various computational design tools considering functionality of objects. For example, researchers have focused on structural strength [Lu et al. 2014; Stava et al. 2012], stability [Bächer et al. 2014; Prévost et al. 2013], or elasticity [Schumacher et al. 2015]. Many of previous studies leverage physical simulation to analyze the functionality of objects and to generate functional designs.

However, it is sometimes difficult to simulate functionality with fully analytic approaches; for this situation, data-driven approaches have been taken to capture complex physical phenomena and material parameters. For example, Umetani et al. [Umetani et al. 2014] proposed a data-driven aerodynamic simulation of hand-launched glider airplanes, and then utilized it in an airplane design tool. They gathered a sample set of glider flight trajectories and learned the relationship between the forces on the wings and wing shapes.

Data-driven approaches are also used to predict human’s perception. Lau et al. [Lau et al. 2016] presented a perceptual model for predicting, given 3D shapes, which areas are more likely to be touched by human. They gathered a large-scale training data using crowdsourcing and utilized a deep learning technique to learn such a perceptual model. Piovarci et al. [Piovarči et al. 2016] proposed a perceptual model for the compliance of nonlinearly elastic objects. To construct the model, they conducted a psychophysical experiment in which a participant compared the compliance of various 3D-printed cubes, and then they evaluated various computational models that predict perceived compliance.

In this work, we construct a mapping from the mass properties of a hand-held object to its perceived shape to design a VR controller. For this, we leverage a data-driven approach in which we collected empirical data of perceived shapes for various hand-held objects and learn a suitable mathematical representation for the mapping. To our knowledge, this is the first attempt to model human’s haptic shape perception and use it as a computational design criterion.

3 FUNDAMENTALS AND OVERVIEW

The VR controllers used in this study are dedicated hand-held objects that functions as a tool or a hand that a user operates in VR spaces. Based on previous studies in ecological psychology [Burton et al. 1990; Kingma et al. 2004; Pagano et al. 1993; Turvey et al. 1998], we construct a shape perception model that can be utilized to computationally design an appropriate VR controller that reproduces a desired haptic shape perception. With this approach, we

can make a controller with proper haptic shape perception that is smaller and/or lighter than a naively designed controller, *i.e.*, the one shaped exactly like the target virtual object. This is beneficial, for example, when the physical space is limited compared with the virtual environment but users want to handle a relatively large virtual object with suitable haptic perception; this is a common situation in indoor VR systems.

3.1 Assumptions on Shape Perception Model

Based on the previous studies concerning the relationship between the mass properties and the perceived shape [Burton et al. 1990; Kingma et al. 2004; Pagano et al. 1993; Turvey et al. 1998], we assume that there is a mapping from the mass properties of a wielded object to its shape perception.

For a hand-held controller C , let the second moment (*i.e.*, the *moment of inertia*) about the handle position be $\mathbf{I} \in \mathbb{R}^{3 \times 3}$, the first moment (*i.e.*, the *static moment* [Kingma et al. 2004]) about the handle position be $\mathbf{M} \in \mathbb{R}^3$, and the shape that a user perceives when grasping it be S . Based on the previous studies [Burton et al. 1990; Kingma et al. 2004; Pagano et al. 1993; Turvey et al. 1998], we assume that the perceived shape S is determined by the moment of inertia \mathbf{I} and the static moment \mathbf{M} about the handle position. That is, we assume the existence of a *shape perception function*:

$$f : (\mathbf{I}, \mathbf{M}) \mapsto S. \quad (1)$$

In this study, we also put the following assumption about the controller C and its perceived shape S to make the shape perception model tractable.

- (1) A controller C and its perceived shape S are both planar with a constant, sufficiently small thickness.
- (2) A controller C and its perceived shape S are both reflective symmetric with respect to the y - z plane.
- (3) A perceived shape S can be represented as a rectangular thin plate made of a homogeneous material.

Under these assumptions, a perceived shape S is parametrized by its *perceived length* L and a *perceived width* W . Although these assumptions may sound strong, it is sufficient to verify our approach, since many hand-held tools can be seen as 2-dimensional planar symmetric shapes.

We define the *handle coordinate system* using the handle position and the handle axes, where the center of the handle is the origin, the handle axis y is parallel to the handle, and the handle axis z is perpendicular to the planar surface of the controller (see the inset figure). In this work, we assume that the length of the handle is approximately 10 cm.

Under these assumptions, a controller C need not be rectangular, but its moment of inertia \mathbf{I} always aligns with the axes (*i.e.*, $\mathbf{I} = \text{diag}(I_x, I_y, I_z)$) and its static moment has only one non-zero entry (*i.e.*, $\mathbf{M} = (0, M_y, 0)$). In addition, as the controller is thin, we have $I_z = I_x + I_y$. As a result, the shape perception function can be

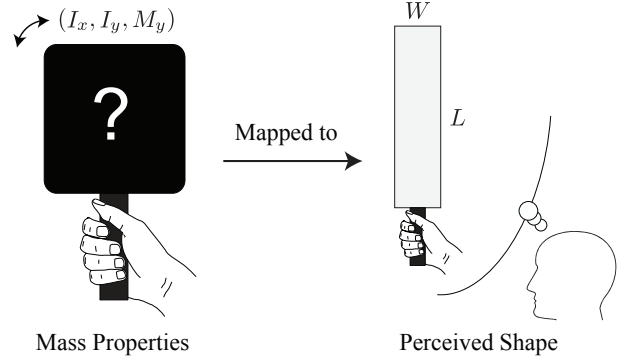


Figure 3: Illustration of the shape perception function that maps the mass properties to the perceived shape. Here, the mass properties are described by three parameters: I_x, I_y (the moment of inertia), and M_y (the static moment). The perceived shape is parametrized using the perceived length L and the perceived width W .

re-written as

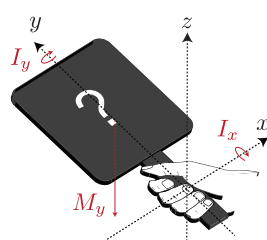
$$f : (I_x, I_y, M_y) \mapsto (L, W). \quad (2)$$

Figure 3 illustrates the shape perception model. To construct the function f , we took a data-driven approach; we collected a set of paired data between a controller with a mass properties (I_x, I_y, M_y) and its perceived shapes (L, W) . For data collection, we conducted an experiment in which participants were asked to wield a set of sample controllers $\{C_i^{\text{sample}}\}$ in a VR environment and to determine their perceived lengths and widths $\{(L_i, W_i)\}$ without seeing their actual appearances. By leveraging function regression techniques on these data, we constructed the function f . Details of the data collection and the function construction are described later.

3.2 Designing Controller using the Shape Perception Model

Using the shape perception function f , we can predict a perceived shape $(L, W) = f(I_x, I_y, M_y)$ for an arbitrary controller C . To design a VR controller, we solve an *inverse* problem for this prediction; given a target shape perception $S^{\text{target}} = (L^{\text{target}}, W^{\text{target}})$, where L^{target} is a target perceived length and W^{target} is a target perceived width, we want to find an optimal controller design C^* whose perceived shape $f(I_x^*, I_y^*, M_y^*)$ is as similar to $(L^{\text{target}}, W^{\text{target}})$ as possible.

Our design workflow is as follows. First, a user inputs the target virtual model and specifies its handle, from which our design system defines the target shape perception $S^{\text{target}} = (L^{\text{target}}, W^{\text{target}})$. Next, the user can specify the maximum and minimum size constraints of the resulting controller. Then, our system automatically solves an optimization problem in which, intuitively, the distance between the target shape S^{target} and the predicted perceived shape is minimized while satisfying the constraints. The system then outputs a CAD data for the optimal controller design C^* , which is easy to fabricate using a laser cutter or a 3D printer. Details of these procedures are explained later.



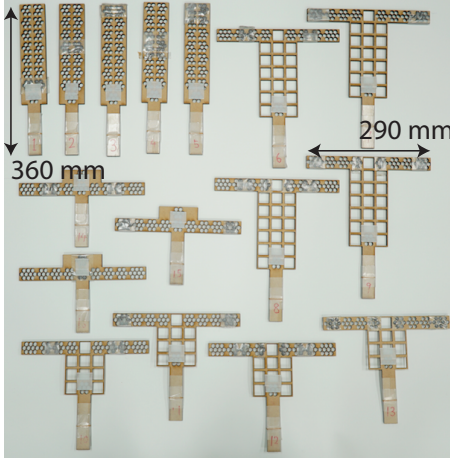


Figure 4: Sample controllers used in the data aggregation experiment.

4 SHAPE PERCEPTION MODEL

We collected data on the perceived length and width (L , W) of various physical controllers with a certain mass properties (I_x , I_y , M_y). These data are later used to regress the shape perception model.

4.1 Collecting Perceived Shape Data

4.1.1 Sample Controllers. Sixteen sample controllers $\{C_i^{\text{sample}}\}$ ($i = 1, \dots, 16$) with various mass properties $\{(I_{xi}, I_{yi}, M_{yi})\}$ were prepared, as shown in Figure 4. The sample controllers were made of a 5.5-mm thick medium-density fibreboard (MDF), and multiple 9-mm diameter lead weights are attached on them in various ways. The handle for all controllers is a 100 mm \times 30 mm rectangle wrapped in curing tape to avoid giving any tactile clue about the controller material of the controllers to participants. The maximum size of the controllers was limited to 360 mm in length and 290 mm in width, and the maximum mass was set to 124 g so as to avoid danger when swinging them in the room. The deflection when swinging these sample controllers was negligibly small. For the details of the mass properties of the sample controllers, see the supplemental material.

4.1.2 VR System. In the previous studies on evaluation of perceived shapes [Burton et al. 1990; Kingma et al. 2004; Pagano et al. 1993; Turvey et al. 1998], participants were blindfolded during wielding objects. Since we want to model the perceived shape which is later used for VR applications, we aggregated data of perceived shapes in a virtual environment. We developed a VR system for this purpose in which participants handle a physical controller and resize its virtual shape so that the haptically perceived shape is as close to the virtual appearance as possible. The system consists of an head-mounted display (HMD, the Oculus Rift DK 2), motion capture cameras (Optitrack Flex 13), a PC, a game controller (Xbox 360 controller), and sample controllers $\{C_i^{\text{sample}}\}$. Tracking markers were attached to the HMD and the sample controllers, and 5 motion capture cameras (Optitrack Flex 13) were placed around the

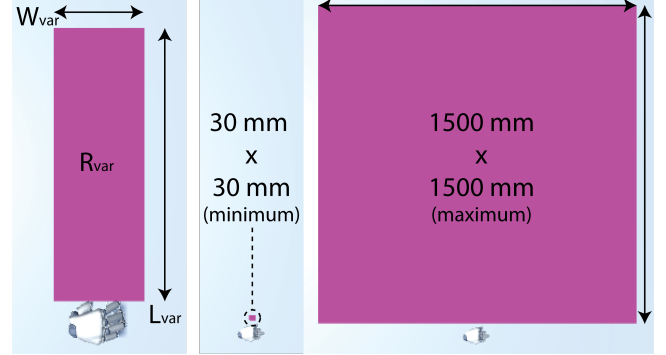


Figure 5: Evaluation model in VR (left) that the users see on the position of the sample controller. Participants adjust the length L_{var} and the width W_{var} of the model. The model is initialized with either the minimum size (center) or the maximum size (right)

2 m \times 2 m working space to obtain the position and the posture of the participant's HMD and the sample controllers. Through the HMD, participants can see a virtual hand and a virtual handle of the same size and position as the actual handle position, which they can move naturally. To evaluate the perceived shape when wielded, a *variable evaluation model* R_{var} was placed and displayed on the tip of the virtual handle. This model has a variable length L_{var} (30 mm $\leq L_{\text{var}} \leq$ 1500 mm) and a variable width W_{var} (30 mm $\leq W_{\text{var}} \leq$ 1500 mm) with constant thickness 5.5 mm (Figure 5). Participants can change the length L_{var} and width W_{var} of the evaluation model R_{var} using the game controller.

4.1.3 Procedure. Participants were asked to sit on a chair, wear an HMD, hold the game controller with their non-dominant hand, and grab the handle of the selected controller with their dominant hand. We selected one of the sample controllers, C_i^{sample} , and displayed R_{var} in the virtual environment. Evaluation model R_{var} has two initial sizes. One of them is the minimum size ($L_{\text{var}}, W_{\text{var}} = (30 \text{ mm}, 30 \text{ mm})$) and the other is the maximum size ($L_{\text{var}}, W_{\text{var}} = (1500 \text{ mm}, 1500 \text{ mm})$). Participants began their evaluation with one of the two. Figure 6 shows a participant and their view in the virtual environment. We chose magenta for the color of the evaluation model R_{var} because an expansive or contractive color would affect participant's size perception.

Participants estimate the size of C_i^{sample} while wielding it in various directions, adjusting the L_{var} and W_{var} to the size that they perceive using the game controller. In the experiment instructions, we requested the participants to wield a sample controller in various direction (away from their body), to touch only the handle, and to assume the same material for all the controllers. When the evaluation of the participants ($L_{\text{var}}, W_{\text{var}}$) was confirmed, we recorded them as (L_i, W_i) , and retrieve the controller from the participants.

Evaluations were performed twice for each pair of a sample controller and initial size (in total, $16 \times 2 \times 2 = 64$ times) in the random order. Each evaluation was limited to 30 seconds, and a 2-minute break was inserted in every 16 evaluations. When starting and resuming the evaluation, participants wielded the reference

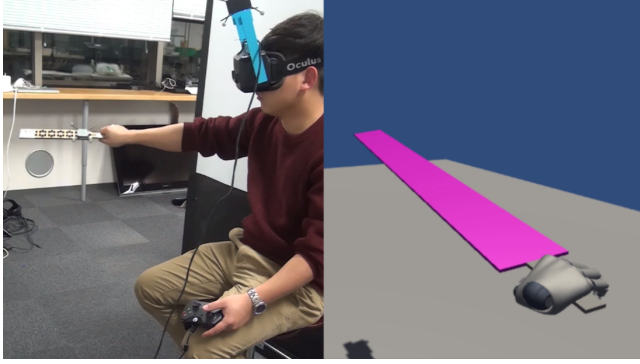


Figure 6: A participant welding a sample controller (left) and their view in the virtual environment (right).

Table 1: Prediction errors with different regression models: linear (LR), quadratic (QR), and Gaussian process (GPR) regressions.

	LR	QR	GPR
Error in L [mm]	117.5	116	115.9
Error in W [mm]	99.2	98.5	97.9

controller which has the same actual shape as the VR appearance to control the material assumptions.

For this experiment, 10 participants were gathered, including 2 women and 2 left-handed people and ranged in age from their 20s to 40s. There were 64 evaluations for each person, so we obtained $64 \times 10 = 640$ evaluation data pairs $\{(I_{xi}, I_{yi}, M_{yi}), (L_i, W_i)\}$.

4.2 Regression Models and Results

Using the 640 data pairs, we performed regression analysis to construct a mapping from the mass properties (I_x, I_y, M_y) to the perceived length and width (L, W) . For regression model selection, we tested *linear regression* (LR), *quadratic regression* (QR), and *Gaussian process regression* [Rasmussen and Williams 2006] (GPR), and compared their prediction performances. Figure 7 visualizes the regression results. Note that these results are not contradictory to the report by Turvey [Turvey 1996], which suggests that L is proportional to I_x, I_y^{-1} , and M_y , and W is proportional to I_x^{-1} and I_y . Table 1 lists the prediction errors of these three regression models. We calculated the prediction errors with the *leave-one-out cross-validation* strategy, where each sample controller is left out once. Although GPR has the smallest prediction errors, there is little difference among these three models; thus we decided to use the function constructed with linear regression (LR) in this study for simplicity.

5 DESIGN SYSTEM

In this section, we describe our design system for designing custom VR controllers, in which we utilize the shape perception model built in the previous section. Figure 8 shows an overview of the system workflow. The input for our system consists of the target

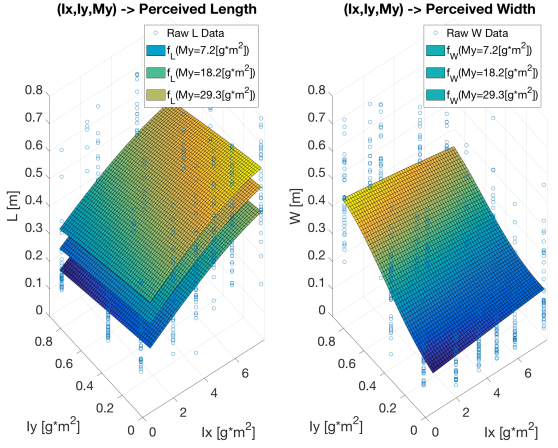


Figure 7: Visualization of the perceptual shape function $f : (I_x, I_y, M_y) \mapsto (L, W)$ constructed by Gaussian process regression (GPR).

virtual object and the target size constraint. After some automatic computation, the system outputs a CAD data for a VR controller that can be fabricated by the user. In the following subsections, we define this input more specifically, and then describe the details of the automatically generated design.

5.1 User Input

A design session begins with a user's specification of the 3D shape model of the target hand-held virtual object. The user must also specify a handle part for grasping. From this information, the system defines the target shape S^{target} ; the target shape is defined with the maximum length L^{target} along the handle axis y from the handle position, and the maximum width W^{target} along the handle axis x . Next, the user can specify a size constraint, which is explained in the next subsection. Finally, the user must also specify the density of the base material ρ for fabrication and the density $\rho'(> \rho)$ of additional weights, which are used in the later optimization step.

5.2 Size Constraint

The user can specify a size constraint; by controlling a rectangle in the interface, the user can specify a rectangular design region $\Omega = \{(x, y) \mid x_{\min} \leq x \leq x_{\max}, y_{\min} \leq y \leq y_{\max}\}$. This will be used in the later computation so that the resulting controller fits within this region. In addition, we also set a constraint that the mesh vertices of the handle part will not be moved in the later computation. As the handle is the only part of the controller that the user touches, they notice large contradictions between the actual and virtual handle shapes; thus, we preserve its shape. Note that the curvature of the other parts' outline also follows the original shape while transformed in case a user unexpectedly touch parts other than the handle. Optionally, instead of specifying size requirements, the user can directly specify an arbitrary shape model for the output model.

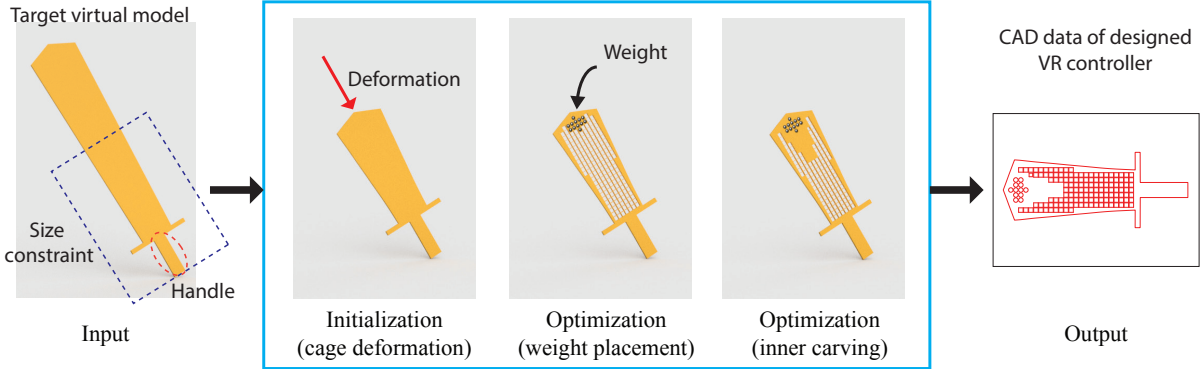


Figure 8: System workflow. The user input consists of the 3D shape model of the target hand-held virtual object, the handle part, and the target size constraint. The output is a CAD data of the designed VR controller for fabrication. The system computes the following 3 steps: The first step is cage deformation, which generates an initial solution that satisfies the size constraints, the second step is weight placement, in which the design is optimized using additional weights, and the third step is inner carving, in which the design is further refined by placing holes.

5.3 Shape Perception Cost

We require the perceived shape of the controller to be close to target shape S^{target} , that is, the perceived length L and width W should be close to the target length L^{target} and width W^{target} , respectively. We define a *shape perception cost* E_S as the squared distance of the perceived scale and the target scales. Since the perceived length and width are computed through the shape perception function, this shape perception cost is also a function of the mass properties:

$$E_S = E_L + E_W, \quad (3)$$

where

$$E_L = \|f_L(I_x, I_y, M_y) - L^{\text{target}}\|^2, \quad (4)$$

$$E_W = \|f_W(I_x, I_y, M_y) - W^{\text{target}}\|^2. \quad (5)$$

5.4 Mass Cost

It is sometimes desirable to reduce the burden on the user and the material cost. Thus, we incorporate a cost term that tries to reduce the mass m of the controller C to the optimization. This *mass cost* is represented as

$$E_m = m. \quad (6)$$

5.5 Optimization

To obtain an optimal controller design, the system solves the following minimization problem:

$$C^* = \arg \min_C \{w_S E_S + w_m E_m\} \quad (7)$$

under the size constraint (*i.e.*, all the vertices are in Ω), where w_S and w_m are the weights for controlling the effects of these cost functions, for which the user can freely provide the values.

To solve the above design optimization, our system utilizes techniques similar to those presented by Bächer et al. [Bächer et al. 2014], which consists of (1) *cage deformation*, (2) *weight placement*, and (3) *inner carving*. Cage deformation generates an initial solution that satisfies the size constraint, weight placement minimizes

the costs with respect to the placement of additional weights, and inner carving further refines the optimization with respect to the placements of holes.

5.5.1 Setting an Initial Solution by Cage Deformation. To get an initial solution that satisfies the size constraint, our system deforms the target shape. As a deformation strategy, we use *bounded biharmonic weights* [Jacobson et al. 2011]. Specifically, our system generates a set of *control points* around the controller mesh, and then moves these points into the user-specified bound Ω . In this deformation process, the system ensures that the mesh vertices of the handle part are not updated. This provides a deformed model that can be used as the starting point of the later minimization steps. Note that, when the user specifies the output controller shape directly, this step is simply skipped.

5.5.2 Optimization by Weight Placement. To achieve the desired mass properties, we use a heavier material (*e.g.*, metal) for additional weight. Although it is possible to fabricate arbitrary shapes with metal and combine them [Bächer et al. 2014], this is too difficult for most end users. Therefore, we considered attaching pre-manufactured metal balls on the base controller.

The system first discretizes the whole shape with regular 2-dimensional grids (see Figure 9). The size of a grid cell is 10 mm \times 10 mm. With these grid cells, the system later computes the weight placement and the inner carving. Since these grid cells are used for inner carving as well, we set a certain margin (~ 5 mm) from the outline to the grid cells so that the mesh model can be fabricated safely even when the cells are carved. Before the computation of weight placement and inner carving, since we want to reduce unnecessary mass as much as possible, the grid cells are uniformly carved with 9 mm \times 9 mm rectangular holes. This is the maximum carving size for each grid cell to maintain the rigidity.

Although this weight placement is a discrete optimization problem, we approximate it as a continuous optimization problem. To each grid cell, we set *weight density ratios* $\alpha_k \in [0, 1]$ ($k =$

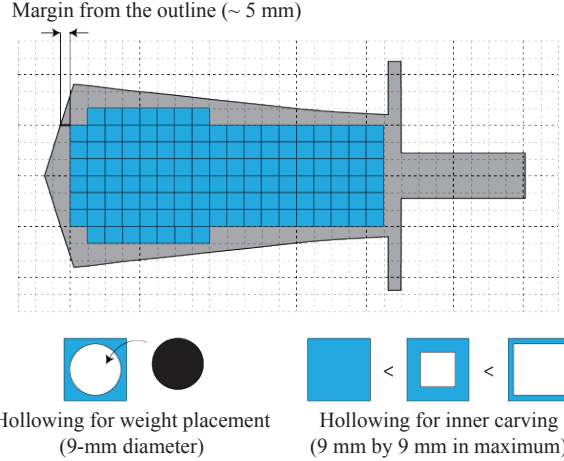


Figure 9: Illustration of the 2-dimensional regular grid on the controller model used for optimization steps. The size of each grid cell is 10 mm × 10 mm and has a certain margin from the outline mesh. During optimization, cells are hollowed either for the weight placement or for the inner carving. For weight placement, a cell is carved with a 9-mm-diameter circle. For inner carving, a cell is carved with a 9 mm × 9 mm rectangle at maximum.

1, ..., #cells). Suppose we replace the cells with the weight material with density ratio α_k ; then, the mass of the whole controller s' can be represented with the mass of the carved mesh s , the weight density ratios α_k , the ratio of weight material to base material ρ_w , and the mass of each cell s_k : $s' = s + \sum_k \alpha_k \rho_w s_k$. Since the derivative of the mass properties with respect to α_k is analytically calculated, we can efficiently solve the optimization problem with respect to the weight density ratios $\{\alpha_k\}$ using the L-BFGS method [Liu and Nocedal 1989] (a gradient-based optimization algorithm) to obtain the optimal density distribution. After obtaining the continuous valued result, the system determines whether a metal ball should be placed or not for each cell by simple thresholding.

5.5.3 Optimization by Inner Carving. Although the weight placement step already provides a good optimization solution (Equation 7), it is possible to further refine the solution and achieve a smaller cost function value with the inner-carving step. To refine the optimization, the system adjusts the density distribution by modifying the controller's inner structure. While there are sophisticated methods for modifying inner structures (e.g., [Bächer et al. 2014; Schumacher et al. 2015]), here we adopt a simple method; the whole shape is divided using a 2-dimensional regular grid as used in the previous subsection and each grid cell is carved in accordance with its *carving ratio*. To each grid cell, we set carving ratios $\beta_k \in [0, 1]$ ($k = 1, \dots, \#cells$). The carving ratio indicates how much the system carves the grid cell when the controller is fabricated. A carving ratio of 1 means that the corresponding grid cell is completely empty, and 0 means it is not carved at all. Thereby the mass s' of the whole mesh can be denoted by the mass of the outline mesh s , the carving ratios β_k , and the mass of each cell s_k : $s' = s - \sum_k \beta_k s_k$. The derivative of the mass properties with respect

to $\{\beta_k\}$ can be analytically calculated, so we solve the optimization with respect to the carving ratios $\{\beta_k\}$ using the L-BFGS method [Liu and Nocedal 1989] again. After obtaining the optimal carving ratios, the system carves each cell by a square such that the mass of the carved cell is proportional to the obtained carving ratio (see Figure 9, Bottom left). We set an upper bound of the carving ratio for the optimization to be 0.81 so that the the maximum hole size for each grid cell is a 9 mm × 9 mm square.

6 RESULTS

We designed several hand-held VR controllers using our system and conducted a user study to validate that the designed controllers present the target shape perception.

6.1 Designed Controllers

Figure 10 shows VR controllers designed with our system. All our models were fabricated using a laser cutter with an MDF and 9-mm-diameter lead weights are placed on them. Our system can produce a controller that have a large perceived length and a small perceived width. On the Sword model, weights placement is concentrated on the tip (Figure 10, Left). Our system can also produce a controller that have a large perceived width. On the Tennis model, weights placement is widely distributed to represent the wide shape of the original model (Figure 10, Center). Our system can allows user to arbitrarily specify the handle position. On the Guitar model, the handle is specified on the neck and the body is transformed while the head is preserved (Figure 10, Right). The length of each designed controller is almost half size in comparison with its original length (Sword: 57.65%, Tennis racket: 51.61%, Guitar: 55.0%).

6.2 User Study

We conducted a user study to evaluate how successfully the controllers designed with our system can present the intended shape perception to the users in a VR environment.

6.2.1 Test Controllers. We prepared five VR controllers (*test controllers* C_i^{test} ($i = 1, \dots, 5$)) designed for different visual shapes (*test visual shapes* S_i^{test} ($i = 1, \dots, 5$)) using our system. Figure 11 shows the test controllers and the test visual shapes, and Table 2 shows the details of the test visual shapes. The test controllers were fabricated using laser-cut 5.5-mm-thick MDF frames and 9-mm-diameter lead weights. The outer shapes were the same for all the controllers, with a handle of 80 mm × 30 mm and frame outline of 260 mm × 200 mm. A curing tape was wrapped around the handle so that the participants could not guess its material from the surface texture. Because the prediction errors of the shape perception function are about 11 cm in length and about 10 cm in width (Table 1), the designed perceived shapes differed at least by 10 cm in either the width or the length.

6.2.2 VR System Setup. The system used for the experiment is almost the same as that used in the data aggregation experiment. In addition, we placed a table containing several controllers, in front of the chair on which participants sit, which was also displayed in the virtual environment as well.

6.2.3 Procedure. Each of the participant sat on a chair and wore an HMD. Tracking markers were attached to all the test controllers,



Figure 10: VR controllers designed with our system: Sword (Left), Tennis racket (Center), and Guitar (Right). For each pair, the target virtual object is shown in the left, and the designed controller is shown in the right.

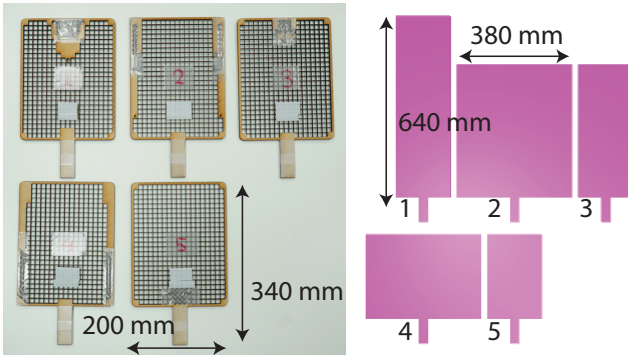


Figure 11: Test controllers designed for the user study (left) and test visual shapes seen in the virtual environment (right, with reduced scale compared to the controller). The red numbers on the controller show the index i for C_i^{test} and the numbers next to the visual shape show the index i for S_i^{test} . The pair of a controller and its assumed perceived shape are placed in the corresponding positions. 9-mm diameter lead weights are placed on the test controllers. The white Velcro is used to attach tracking markers.

Table 2: The length and width of the test visual shapes S_i^{test} .

	S_1^{test}	S_2^{test}	S_3^{test}	S_4^{test}	S_5^{test}
Length [mm]	640	480	480	320	320
Width [mm]	180	380	180	380	180

which were arranged in a random order on the table so that the participants were unaware of their placement. We selected one of the perceived shapes and superimposed its appearance on all the controllers. The participant picked up the controllers with their dominant hand in any order, compared his perception with that of the current visual shape, and selected the one that matched best. Before the test starts, participants are instructed to move the controllers in various directions for the comparison. This evaluation was carried out four times for each visual shape (twenty times in total) in a random order. Participants consist of 5 right handed male people in their 20's.

Table 3: Each row shows ratios of the test controllers C_i^{test} answered for a test visual shape S_i^{test} . The cells with bold characters shows a pair where the perceived shape of the test controller matches the test visual shape.

	C_1^{test}	C_2^{test}	C_3^{test}	C_4^{test}	C_5^{test}
S_1^{test}	40%	30%	30%	0%	0%
S_2^{test}	20%	65%	0%	15%	0%
S_3^{test}	5%	10%	70%	15%	0%
S_4^{test}	0%	30%	5%	65%	0%
S_5^{test}	0%	5%	35%	5%	55%

6.2.4 Result and Discussion. Table 3 shows the percentage of the test controllers C_i^{test} answered for the test visual shapes S_i^{test} . Each row shows the rate at which each test controller was selected when the test visual shape was displayed. For each test visual shape, the corresponding test controller was selected the most frequently among all the controllers. It suggests that the controllers designed with our system successfully presented the intended shape perception to the users.

Most of the misjudgments were made to the controllers that have the same length or width as the intended one or to the controllers that have similar scales (e.g., C_1^{test} , C_2^{test} and C_3^{test} for S_1^{test} , C_2^{test} and C_4^{test} for S_4^{test} , and C_3^{test} and C_5^{test} for S_5^{test}). For the test virtual shape S_1^{test} , both C_2^{test} and C_3^{test} were selected many times while C_1^{test} remains only 40 %. Note that C_1^{test} has a little weak structure due to the inner carving and it could slightly bend when participants swing it strongly, which might have affected the shape perception.

7 LIMITATIONS AND FUTURE WORK

We proceeded with experiments with a simplified shape perception model as the first step in exploring our concept. To extend this work and handle more complex shape perception, certain technical challenges should be addressed.

Simplification to Symmetric Planar Objects. In this work, we specifically focused on the perception of symmetric planar objects. Of course, there are objects that does not fit in this scope. As our principal concept described in Equation 1 is general and not specific to symmetric planar objects, we believe that more complex

shapes could be handled by extending the parametrization of our perception model. For example, perception of non-symmetric objects could be parametrized by the distance of the center of mass (CoM) from the handle axis in addition to the width and length. Similarly, full 3D objects would be modeled within our concept by considering additional dimensions such as thickness and the position of CoM. Shape perception models for these cases could be computed from additional data sets aggregated in a similar way as our experiment. However, adequate parametrizations and effective sampling strategies for larger dimensions (e.g., active learning) are non-trivial, which we would leave as future work.

Air Resistance and Deflection. We assumed that shape perception is solely correlated with objects' mass properties of objects and ignored the influence of air resistance or deflection. Such effects were negligible for small or mesh-structured objects. However, in some cases, air resistance and deflection could greatly influence the impression of the perceived shape. For example, it is easy to imagine that the feeling of wielding a paper fan is affected by air resistance and deflection. To represent the impression of wielding such objects, we must incorporate such effects into the shape perception model.

Dynamic Shape Perception. Our design tool focuses on a *static* hand-held controller with a single haptic shape perception; the controller never changes its shape. However, our perceptual model can be applied to *dynamic* perceptual shape modification. For example, it is possible to dynamically change the mass parameters and shape perception accordingly, by moving the controller's inner weights. By employing such mechanisms on a controller, we can render different shape perceptions without changing the controller.

8 CONCLUSION

We presented a novel computational design method for hand-held VR controllers that uses a haptic shape illusion. Inspired by the studies in ecological psychology, we modeled a mapping from the mass properties of the controller to its perceived shape by a data-driven approach. We prepared controllers with a variety of shapes and mass properties and conducted an experiment in which participants reported the perceived shape of each controller. We constructed a shape perception model using regression techniques on the aggregated data and implemented a design system that can computationally design hand-held VR controllers that could reproduce desired shape perceptions. We conducted a user study with the designed controllers and showed that many participants illusorily perceived the intended shapes irrespective of the controller's actual appearance.

REFERENCES

- Tomohiro Amemiya, Hideyuki Ando, and Taro Maeda. 2008. Lead-me Interface for a Pulling Sensation from Hand-held Devices. *ACM Trans. Appl. Percept.* 5, 3, Article 15 (Sept. 2008), 17 pages. <https://doi.org/10.1145/1402236.1402239>
- Mahdi Azmandian, Marj Hancock, Hrvoje Benko, Eyal Ofek, and Andrew D. Wilson. 2016. Haptic Retargeting: Dynamic Repurposing of Passive Haptics for Enhanced Virtual Reality Experiences. In *Proc. CHI '16*. 1968–1979. <https://doi.org/10.1145/2858036.2858226>
- Moritz Bächer, Emily Whiting, Bernd Bickel, and Olga Sorkine-Hornung. 2014. Spin-it: Optimizing Moment of Inertia for Spinnable Objects. *ACM Trans. Graph.* 33, 4 (2014), 96:1–96:10. <https://doi.org/10.1145/2601097.2601157>
- Hrvoje Benko, Christian Holz, Mike Sinclair, and Eyal Ofek. 2016. NormalTouch and TextureTouch: High-fidelity 3D Haptic Shape Rendering on Handheld Virtual Reality Controllers. In *Proc. UIST '16*. 717–728. <https://doi.org/10.1145/2984511.2984526>
- Gregory Burton, M. T. Turvey, and H. Yosef Solomon. 1990. Can shape be perceived by dynamic touch? *Perception & Psychophysics* 48, 5 (01 Sep 1990), 477–487. <https://doi.org/10.3758/BF03211592>
- James Jerome Gibson. 1966. *The Senses Considered as Perceptual Systems*. Houghton Mifflin.
- Alec Jacobson, Ilya Baran, Jovan Popović, and Olga Sorkine. 2011. Bounded Biharmonic Weights for Real-time Deformation. *ACM Trans. Graph.* 30, 4, Article 78 (July 2011), 8 pages. <https://doi.org/10.1145/2010324.1964973>
- Idarts Kingma, Rolf van de Langenberg, and Peter J Beek. 2004. Which mechanical invariants are associated with the perception of length and heaviness of a nonvisible handheld rod? Testing the inertia tensor hypothesis. *Journal of Experimental Psychology: Human Perception and Performance* 30, 2 (2004), 346–54. <https://doi.org/10.1037/0096-1523.30.2.346>
- Manfred Lau, Kapil Dev, WeiQi Shi, Julie Dorsey, and Holly Rushmeier. 2016. Tactile Mesh Saliency. *ACM Trans. Graph.* 35, 4, Article 52 (July 2016), 11 pages. <https://doi.org/10.1145/2897824.2925927>
- D. C. Liu and J. Nocedal. 1989. On the Limited Memory BFGS Method for Large Scale Optimization. *Math. Program.* 45, 3 (Dec. 1989), 503–528. <https://doi.org/10.1007/BF01589116>
- Lin Lu, Andrei Sharf, Haisen Zhao, Yuan Wei, Qingnan Fan, Xuelin Chen, Yann Savoye, Changhe Tu, Daniel Cohen-Or, and Baoguan Chen. 2014. Build-to-last: Strength to Weight 3D Printed Objects. *ACM Trans. Graph.* 33, 4, Article 97 (July 2014), 10 pages. <https://doi.org/10.1145/2601097.2601168>
- Thomas H Massie and J Kenneth Salisbury. 1994. The phantom haptic interface: A device for probing virtual objects. In *Proceedings of the ASME winter annual meeting, symposium on haptic interfaces for virtual environment and teleoperator systems*, Vol. 55. Chicago, IL, 295–300.
- Kouta Minamizawa, Souichiro Fukamachi, Hiroyuki Kajimoto, Naoki Kawakami, and Susumu Tachi. 2007. Gravity Grabber: Wearable Haptic Display to Present Virtual Mass Sensation. In *ACM SIGGRAPH 2007 Emerging Technologies*. Article 8. <https://doi.org/10.1145/1278280.1278289>
- S. Nakagawara, H. Kajimoto, N. Kawakami, S. Tachi, and I. Kawabuchi. 2005. An Encounter-Type Multi-Fingered Master Hand Using Circumferential Joints. In *Proc. ICRA '05*. 2667–2672. <https://doi.org/10.1109/ROBOT.2005.1570516>
- H. Omosako, A. Kimura, F. Shibata, and H. Tamura. 2012. Shape-COG Illusion: Psychophysical influence on center-of-gravity perception by mixed-reality visual stimulation. In *2012 IEEE Virtual Reality Workshops (VRW)*. 65–66. <https://doi.org/10.1109/VR.2012.6180884>
- Christopher C. Pagano, Paula Fitzpatrick, and M. T. Turvey. 1993. Tensorial basis to the constancy of perceived object extent over variations of dynamic touch. *Perception & Psychophysics* 54, 1 (01 Jan 1993), 43–54. <https://doi.org/10.3758/BF03206936>
- Michal Piovarčí, David I. W. Levin, Jason Rebello, Desai Chen, Roman Đuričovič, Hanspeter Pfister, Wojciech Matusik, and Piotr Didyk. 2016. An Interaction-aware, Perceptual Model for Non-linear Elastic Objects. *ACM Trans. Graph.* 35, 4, Article 55 (July 2016), 13 pages. <https://doi.org/10.1145/2897824.2925885>
- Romain Prévost, Emily Whiting, Sylvain Lefebvre, and Olga Sorkine-Hornung. 2013. Make It Stand: Balancing Shapes for 3D Fabrication. *ACM Trans. Graph.* 32, 4, Article 81 (July 2013), 10 pages. <https://doi.org/10.1145/2461912.2461957>
- Carl Edward Rasmussen and Christopher K. I. Williams. 2006. *Gaussian Processes for Machine Learning*. MIT Press.
- Jun Rekimoto. 2013. Traxion: A Tactile Interaction Device with Virtual Force Sensation. In *Proc. UIST '13*. 427–432. <https://doi.org/10.1145/2501988.2502044>
- Christian Schumacher, Bernd Bickel, Jan Rys, Steve Marschner, Chiara Daraio, and Markus Gross. 2015. Microstructures to Control Elasticity in 3D Printing. *ACM Trans. Graph.* 34, 4, Article 136 (July 2015), 13 pages. <https://doi.org/10.1145/2766926>
- Ondřej Stava, Juraj Vaneček, Bedřich Benes, Nathan Carr, and Radomír Měch. 2012. Stress Relief: Improving Structural Strength of 3D Printable Objects. *ACM Trans. Graph.* 31, 4, Article 48 (July 2012), 11 pages. <https://doi.org/10.1145/2185520.2185544>
- M. T. Turvey. 1996. Dynamic Touch. *American Psychologist* 51, 11 (November 1996), 1134–1152. <https://doi.org/10.1037/0003-066X.51.11.1134>
- M. T. Turvey, Gregory Burton, Eric L. Amazeen, Matthew Butwill, and Claudia Carello. 1998. Perceiving the width and height of a hand-held object by dynamic touch. *Journal of Experimental Psychology: Human Perception and Performance* 24, 1 (1998), 35–48. <https://doi.org/10.1037/0096-1523.24.1.35>
- Nobuyuki Umetani, Yuki Koyama, Ryan Schmidt, and Takeo Igarashi. 2014. Pteromys: Interactive Design and Optimization of Free-formed Free-flight Model Airplanes. *ACM Trans. Graph.* 33, 4, Article 65 (July 2014), 10 pages. <https://doi.org/10.1145/2601097.2601129>
- André Zenner and Antonio Krüger. 2017. Shifty: A Weight-Shifting Dynamic Passive Haptic Proxy to Enhance Object Perception in Virtual Reality. *IEEE Transactions on Visualization and Computer Graphics* 23, 4 (2017), 1285–1294. <https://doi.org/10.1109/TVCG.2017.2656978>